Influence of different microstructures of the welding zone on the fatigue crack growth behaviour of HSLA steels

B. Maier [1,*], Ch. Guster[1], R. Tichy[2] and W. Ecker[2]

[1] Montanuniversität Leoben, Chair of Mechanical Engineering, Franz-Josef-Strasse 18, 8700 Leoben, Austria
[2] Materials Center Leoben Forschung GmbH, Roseggerstrasse 12, 8700 Leoben, Austria
* Corresponding author: bernd.maier@unileoben.ac.at

Abstract To meet the cost and weight reduction requirements in welded structures, high-strength low-alloy (HSLA) steels are increasingly used in all fields of mechanical engineering. However, in comparison to low-strength steels these materials are more susceptible to notches or initial cracks. Therefore, an extensive investigation of fatigue crack growth behaviour in the different microstructural zones of the heat-affected zone (HAZ) of the weld is necessary for an appropriate lifetime evaluation of welded joints.
For this purpose, fracture mechanics parameters like thresholds and crack growth rates in the different microstructural zones of the HAZ as well as in the base material are characterized by single edge notched bending (SENB) specimens. The different microstructures are reproduced with a Gleeble thermal simulator system using the same heating curves as measured previously during the welding process of a representative joint. The specimens feature the three characteristic microstructural zones of the HAZ (intercritical, fine-grained and coarse-grained zone). The effect of varying stress ratio R on the crack growth threshold and the crack growth curves is also assessed.

Keywords fatigue crack growth, HAZ, microstructures, HSLA

1. Introduction

For cost reduction reasons in mechanical engineering, especially in the field of welded constructions, the use of high-strength steels increases. Low-strength steels are uncomplicated in construction and usage due to notch insensitivity and good-natured crack propagation behaviour, whereas high-strength steels are much more challenging in construction and processing. With rising strength these steels are more susceptible to notches, pores or initial cracks, so the adequate dimensioning of welds made of such steels requires a high degree of knowledge of material-specific values. Although post-welding conditioning like high-impact treatment is common for such welds, the effects of these treatments have been investigated only phenomenologically so far. Especially the shift of the mean stress and its influence on the fatigue behaviour of the different microstructural zones in the heat affected zone of the weld has to be investigated. Whereas the effects of the weld toe can be described with classical stress-based approaches, the effects of pores or initial cracks require a more sophisticated fracture mechanic approach. In corresponding guidelines like the IIW recommendations [1] thresholds of only 2 MPa$\sqrt{m}$ are used, which lies below the effective threshold $\Delta K_{theff.}$. This leads to a high safety factor on one hand, but is in conflict with the principle of lightweight design on the other hand. Furthermore, only the crack propagation behaviour of the base material is well known, while the other microstructural zones of the weld are ignored. So the aim of this work is the investigation of the fatigue crack propagation behaviour in the different characteristic microstructural zones of the HAZ of a welded joint at different stress ratios.

2. Manufacturing of the different microstructural zones

The HAZ of a welded joint can be subdivided into three different zones, where the microstructure differs significantly from that of the base material (Fig. 1). The base material (BM) is a

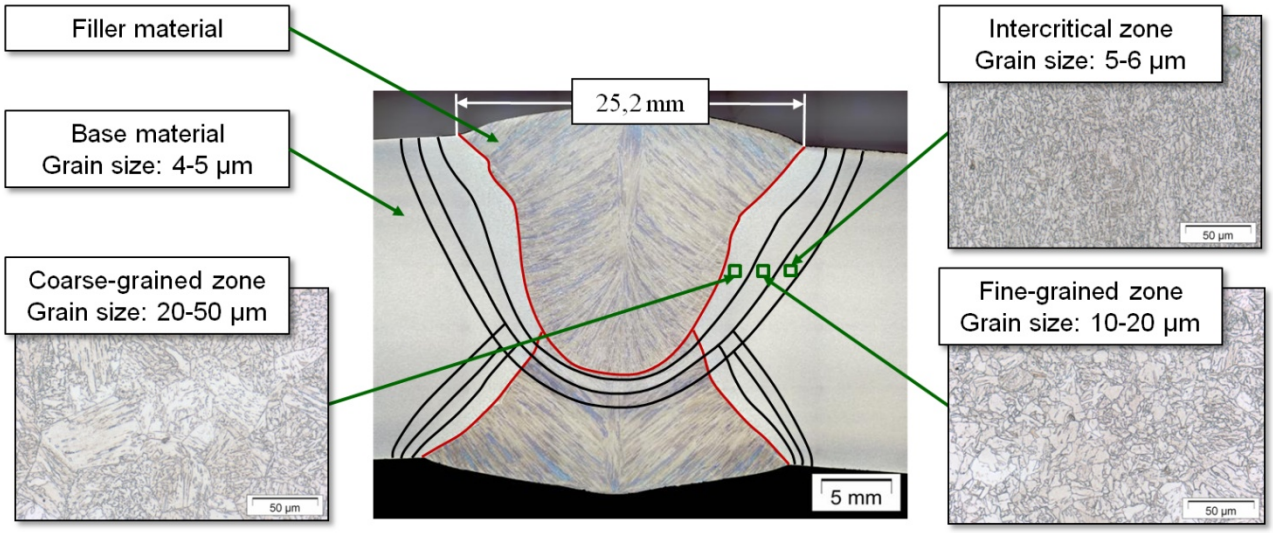

Figure 1. Characteristic microstructural zones of the HAZ of a double-submerged arc-welded joint [3]

thermomechanically rolled high-strength steel with an average grain size of 4-5 µm. The so-called intercritical zone (IZ) has a fine microstructure with an average grain size of about 5 to 6 µm, while in the fined-grained zone (FZ) an average grain size of about 10 to 20 µm was determined. The coarse-grained zone (CZ) shows an average grain size of up to 50 µm. The chemical composition of the base material is shown in Tab.1.

Before reproducing the microstructures it is necessary to get information about the local "heat treatment" due to the welding process for the formation of the characteristic zones of the HAZ. For this purpose metal sheets with a thickness of 20 mm are double-submerged arc-welded to represent the real welding process. For the appropriate measurement of the temperatures sensors are pinned onto the blank sheets in defined distances to the weld (Fig. 2, left). The gathered temperature curves (intercritical zone IZ, fine-grained zone FZ) are shown in Fig. 2 (right).

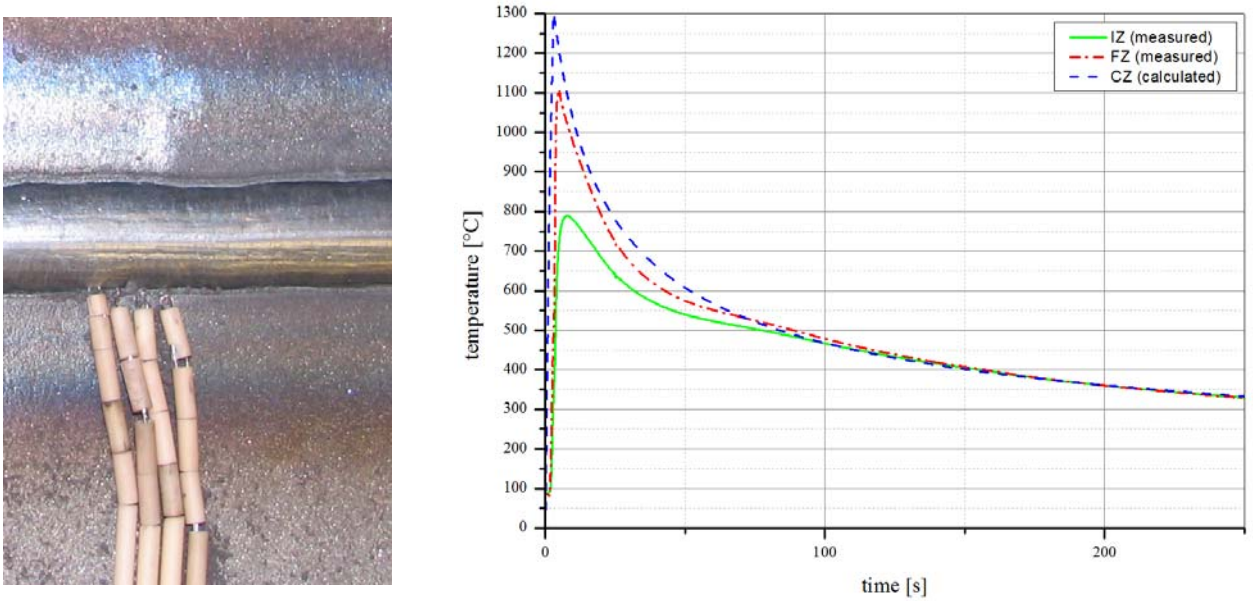

Figure 2. Positioning of the temperature sensors (left) and temperature curves for the heat treatment (right) [3]

Table 1. Chemical composition of the base material [%]

C	Si	Mn	P	S	Al	Cr	Ni	Mo	Cu	V	Nb	Ti
0.05	0.3	1.8	0.009	0.001	0.04	0.2	0.0	0.1	0.0	0.00	0.04	0.01

The temperature curve of the coarse-grained zone (CZ) was calculated according to SEW 088 [2] based on the other measured temperature curves. These heating curves, especially the cooling rates and peak temperatures, are the input for the heat treatment of metal blanks in a Gleeble thermal simulator. With this procedure, blanks with similar microstructures as found in the IZ, FZ and CZ are produced.

After producing these so-called Gleeble blanks, the homogeneity of the resulting microstructures has to be verified. After grinding, polishing and etching of the microsections of the three distinctive zones, they were investigated at different positions across the specimen cross section with optical microscopy and EBSD[1] captures. The results were compared with the results of the investigations of the HAZ of the laboratory weld. As a preliminary result, the microsections differ marginally in grain size, but show a good correlation along the width of the specimen. Additional information from hardness measurements with the Vickers method confirms the overall picture, that the Gleeble blanks exhibit a homogeneous microstructure in the areas of interest and no deviation of crack propagation and fatigue endurance limit due to differing microstructures should occur.

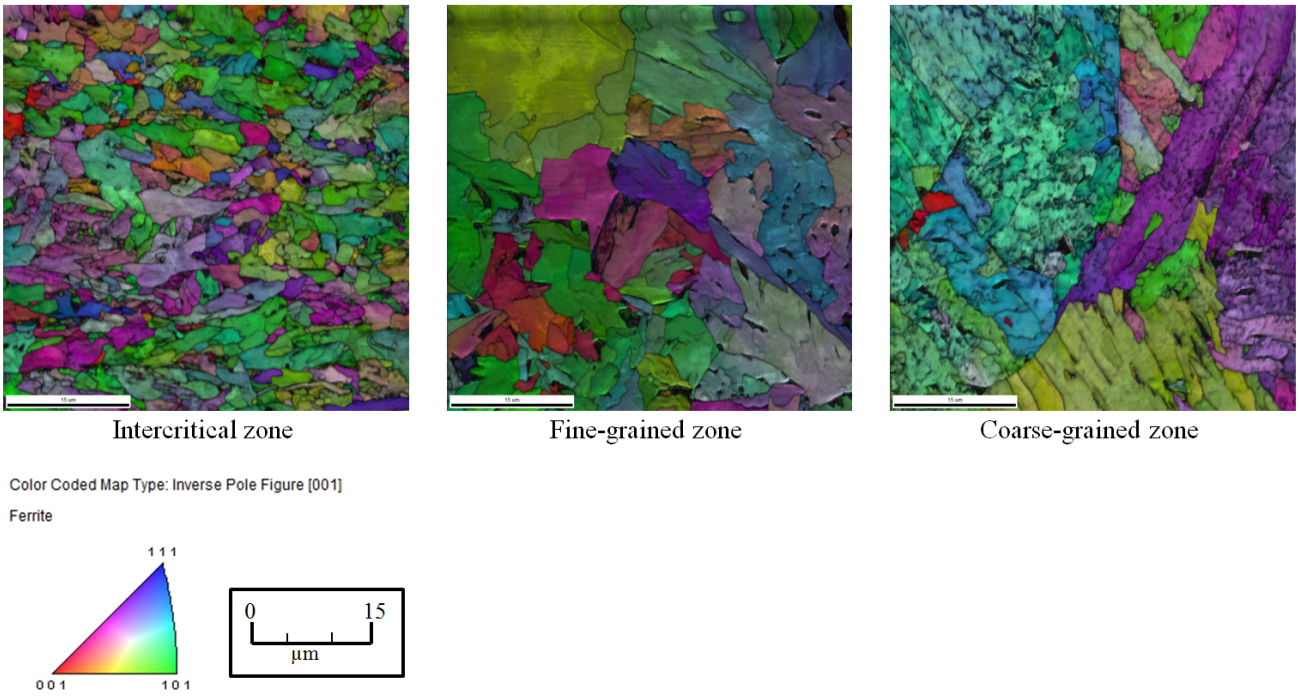

Figure 3. EBSD captures of the different zones

It was also found that due to thermomechanical rolling a distinctive texture orientation is established in the microstructure of the base material. This orientation can also be found in the intercritical zone. Because of the lower temperatures, no microstructural changes occur in this zone. Due to higher temperatures in the FZ and CZ a phase change takes place and the original orientation of the base material is eliminated; the evolution of orientation and average grain size can be seen from Fig. 3.

[1] Electron backscatter diffraction

3. Fatigue crack growth

For the investigation of the crack propagation behaviour, single-edge notched bending (SENB) specimens are used. The tests are performed on a RUMUL Cracktronic resonance testing rig. For crack length measurements a direct-current potential-drop (DCPD) measurement system developed in-house is used. For minimizing the effect of the plastic zone, the so called CPCA testing method is used. This method and its differences to the method according to ASTM [4] are well described in the literature [5]; for the sake of completeness, the general procedure will be described here. The specimens are initially compression pre-cracked for gathering a small plastic zone around the initial crack tip. After this, the specimen is loaded with an initial bending moment resulting in a stress intensity factor higher than the effective threshold ΔK_{theff} but lower than the long-crack threshold ΔK_{th}. The crack will start to grow and will stop after a certain distance due to crack closure effects. Now the bending moment is increased, the same procedure as described before will occur. This procedure is repeated until the stress intensity reaches the long-crack threshold. There the crack will not stop, and the fatigue crack growth curve (FCG) is obtained. For region I of the FCG curve a modified Klesnil-Lukas approach (Eq. 1) and for region II the classic Paris-Erdogan law (Eq. 2) is used. The findings of the different microstructures can be found in Tab. 2 (base material), Tab. 3 (intercritical zone), Tab. 4 (fine-grained zone) and Tab. 5 (coarse-grained zone). Due to missing K_{Ic}-Values fitting of region III has to be skipped. In the following figures the crack propagation curves are only extended without consideration of K_{Ic} until a stress intensity of 50 MPa√m is reached, and then truncated.

$$\frac{da}{dN} = C \cdot \Delta K^{m-p} \cdot \left(\Delta K^{p} - \Delta K_{th}^{p}\right), \tag{1}$$

$$\frac{da}{dN} = C \cdot \Delta K^{m}, \tag{2}$$

Table 2: Crack propagation behaviour of the base material

Specimen	R	ΔK_{th}	C	m
BM-A	0,5	2,92	1,95E-08	2,60
BM-B	0,5	2,90	2,57E-08	2,56
BM-C	0,1	4,40	6,05E-09	2,93
BM-D	0,1	3,56	3,88E-09	3,01
BM-E	-1	13,35	5,85E-10	2,90
BM-F	-1	9,05	2,61E-10	2,98

Table 3: Crack propagation behaviour of the intercritical zone

Specimen	R	ΔK_{th}	C	m
IZ-A	0,5	7,70	5,48E-09	2,87
IZ-B	0,5	7,20	5,40E-09	2,95
IZ-C	0,1	11,90	3,97E-10	3,39
IZ-D	0,1	12,55	3,95E-11	4,25
IZ-E	-1	28,50	3,82E-10	2,59
IZ-F	-1	29,65	3,48E-13	4,28

Table 4: Crack propagation behaviour of the fine-grained zone

Specimen	R	ΔK_{th}	C	m
FZ-A	0,5	4,80	1,86E-09	3,37
FZ-B	0,5	5,30	1,47E-09	3,45
FZ-C	0,1	6,50	3,27E-11	4,41
FZ-D	0,1	6,80	4,19E-12	4,99
FZ-E	-1	19,98	2,44E-13	4,66
FZ-F	-1	17,50	1,10E-13	4,88

Table 5: Crack propagation behaviour of the coarse-grained zone

Specimen	R	ΔK_{th}	C	m
CZ-A	0,5	4,90	1,99E-09	3,29
CZ-B	0,5	4,60	6,37E-09	2,97
CZ-C	0,1	7,05	3,68E-10	3,58
CZ-D	0,1	8,60	2,40E-10	3,73
CZ-E	-1	18,84	1,59E-12	4,33
CZ-F	-1	18,00	3,00E-13	4,76

4. Comparison of the fatigue crack behaviour of the different microstructures

The tabular data of the different microstructures can be found in Tables 2-5; in the following discussion this data will be graphically formatted to demonstrate the differences. As expected the diagrams show a shift from lower thresholds at R=0.5 (Fig. 4) to higher ones at R=0.1 (Fig. 5) and R=-1 (Fig. 6). In general the following trend correlates through all stress ratios: the base material shows the lowest thresholds, followed by the coarse-grained and the fine-grained zone.

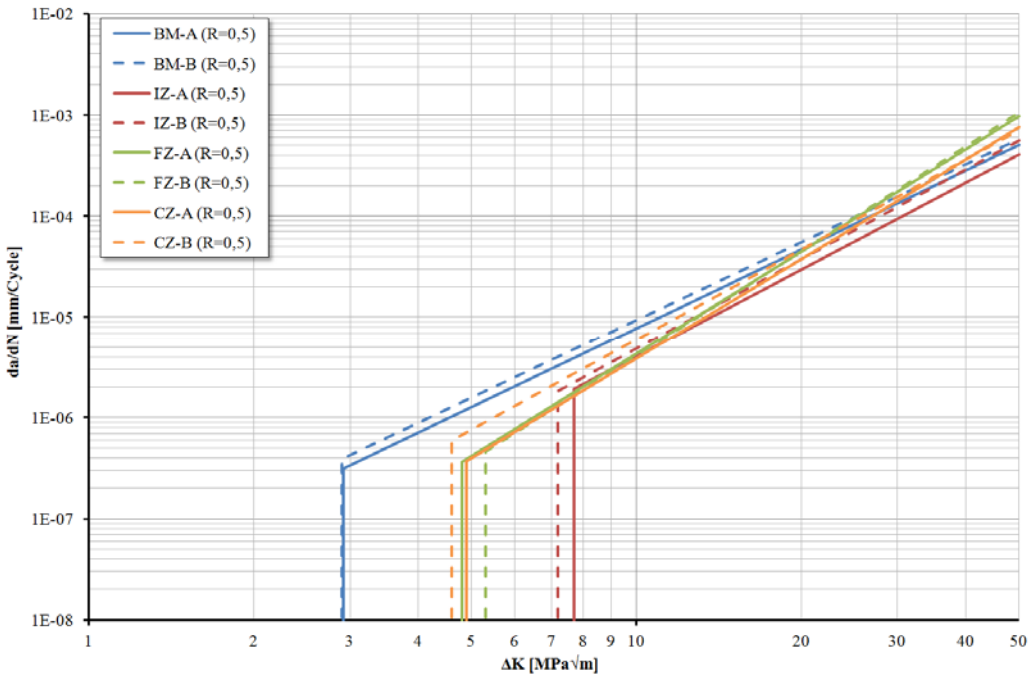

Figure 4. Comparison of the FCG behaviour of the different zones at R=0.5

The intercritical zone shows disproportionately high thresholds in comparison to the other zones, which is due to the long $t_{8/5}$-time of nearly 70 seconds resulting in a soft-annealing of the microstructure and leading to an increase in ductility. The slopes of the Paris-Erdogan regime show values between 2.56 and 4.88. Because of the setup of the crack measurement system (measurement of the potential drop by spring probes) especially the experiments with a stress ratio of R=-1 are hard to execute. The spring probes are losing the contact to the surface of the specimen, in particular at higher amplitudes. Therefore the scatter of the measured voltages increases, leading to a higher scatter of the thresholds and the crack propagation rates.

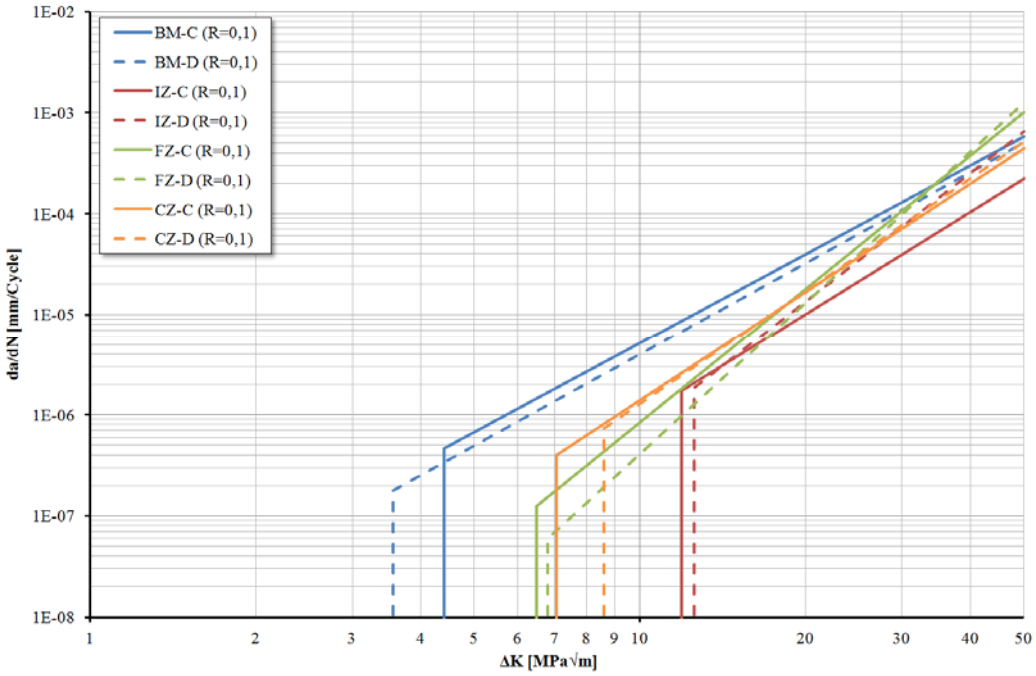

Figure 5. Comparison of the FCG behaviour of the different zones at R=0.1

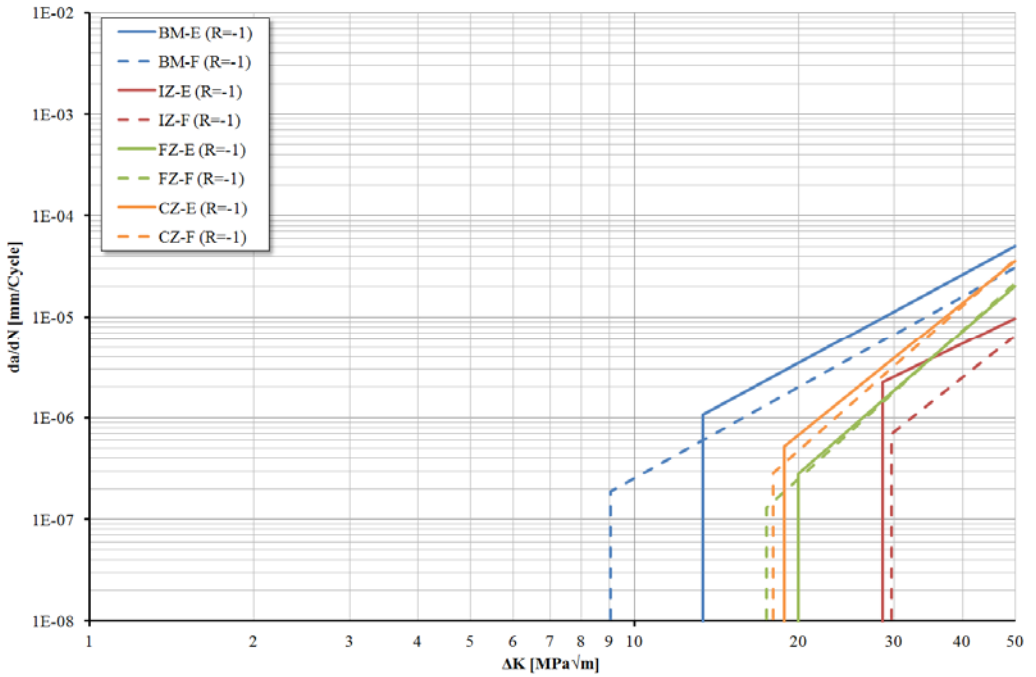

Figure 6. Comparison of the FCG behaviour of the different zones at R=-1

5. Conclusion

The results show that surprisingly, the base material has the lowest thresholds among all microstructures of the HAZ of the representative weld. This could presumably be due to the distinctive texture or the residual stresses in the metal blanks stemming from the rolling process. If no post-weld treatments like machining of the weld or impact treatments are performed, the geometric notch at the weld toe is the crack initiation point. Under cyclic loading, the conservative approach of the low thresholds of 2 MPa√m as a base of a fracture mechanics design approach in the studied case (double-submerged arc-welded with high $t_{8/5}$ times) only makes sense if the geometric notch has a low influence and crack initiation occurs in the base material. With these results it also can be shown how a shift of the stress ratio R influences the crack propagation thresholds within the HAZ. Further investigations concerning the residual stress state in the metal sheet blanks are necessary, however. This work represents an important preliminary contribution to a better understanding and interpretation of different effects due to manufacturing, machining and post-welding processes in the different regions of the HAZ and their influence on the fatigue crack propagation behaviour.

Acknowledgements

Financial support by the Austrian Federal Government and the Styrian Provincial Government, represented by Österreichische Forschungsförderungsgesellschaft mbH and Steirische Wirtschaftsförderungsgesellschaft mbH, within the research activities of the K2 Competence Centre on “Integrated Research in Materials, Processing and Product Engineering”, operated by the Materials Center Leoben Forschung GmbH under the frame of the Austrian COMET Competence Centre Programme, is gratefully acknowledged.

References

[1] A. Hobbacher: Recommendations for fatigue design of welded joints and components, IIW Document IIW-1823-07, December 2008
[2] Technical document SEW 088, Beiblatt 2, 4.Ausgabe, 1993
[3] B. Maier, B. Oberwinkler B., R. Tichy, W. Ecker, Development of a FE-based fracture mechanical method for fatigue life assessment of double-submerged welded pipelines considering residual stresses and local microstructures, Proceedings of the 19th European Conference on Fracture, Kazan, 2012
[4] ASTM E647, Standard Test Method for Measurement of Fatigue Crack Growth Rates, Standards of ASTM International, West Conshohocken, PA
[5] R. Pippan, H.P. Stüwe, K. Golos, A Comparison of Different Methods to Determine the Threshold of Fatigue Crack Propagation, Int. Journal of Fatigue, Vol. 16, 579–582, 1994
[6] J. Kohout, A new function describing fatigue crack growth curves, Int. Journal of Fatigue, Volume 21, 813-821, 1999